

ASYMMETRY IN VELOCITY AND INTENSITY HELIOSEISMIC SPECTRA: A SOLUTION TO A LONG-STANDING PUZZLE

R. NIGAM, A. G. KOSOVICHEV, P. H. SCHERRER, AND J. SCHOU

W. W. Hansen Experimental Physics Laboratory, Stanford University, Stanford, CA 94305-4085; rnigam@solar.stanford.edu,
akosovichev@solar.stanford.edu, pscherrer@solar.stanford.edu, jschou@solar.stanford.edu

Received 1997 June 18; accepted 1998 January 8; published 1998 February 23

ABSTRACT

We give an explanation for the opposite sense of asymmetry of the solar acoustic mode lines in velocity and intensity oscillation power spectra, thereby solving the half-decade-old puzzle of Duvall and coworkers. The solution came after comparing the velocity and intensity oscillation data of medium angular degree l obtained from the Michelson Doppler Imager instrument on board the *Solar and Heliospheric Observatory* with the theoretical power spectra. We conclude that the solar noise in the velocity and intensity spectra is made up of two components: one is correlated to the source that is responsible for driving the solar p -modes, and the other is an additive uncorrelated background. The correlated component of the noise affects the line profiles. The asymmetry of the intensity spectrum is reversed because the correlated component is of a sufficiently large level, while the asymmetry of the velocity spectrum remains unreversed because the correlated component is smaller. This also explains the high-frequency shift between velocity and intensity at and above the acoustic cutoff frequency. A composite source consisting of a monopole term (mass term) and a dipole term (force due to Reynolds stress) is found to explain the observed spectra when it is located in the zone of superadiabatic convection at a depth of 75 ± 50 km below the photosphere.

Subject headings: convection — Sun: interior — Sun: oscillations — turbulence

1. INTRODUCTION

Observations of Duvall et al. (1993) indicated that the power spectra of solar acoustic (p) modes show varying amounts of asymmetry. In particular, the velocity and intensity power spectra revealed an opposite sense of asymmetry. There was scepticism about the result (Abrams & Kumar 1996), and it was even believed to be an error in the experiment. However, the new Michelson Doppler Imager (MDI) data presented here confirm the result and, in addition, allow us to study the variations of asymmetry among modes of various angular degrees and frequencies.

The variations in the asymmetry have important implications in helioseismology, where the eigenfrequencies are generally determined by assuming that the line profile is symmetric and can be fitted by a Lorentzian profile. This leads to systematic errors in the determination of frequencies and, thus, affects the results of inversions.

Several authors have studied this problem theoretically and have found that there is an inherent asymmetry when the solar oscillations are excited by a localized source (Gabriel 1992; Duvall et al. 1993; Roxburgh & Vorontsov 1995; Abrams & Kumar 1996; Nigam, Kosovichev, & Scherrer 1997). Physically, the asymmetry is a result of interference between an outward-directed wave from the source and a corresponding inward-directed wave that passes through the region of wave propagation (Duvall et al. 1993).

However, the precise cause for the asymmetry and its relation to the Sun's acoustic source have not been pinned down in the past. We briefly describe the observations, formulate a theoretical model, and from it suggest an explanation for the difference in the two asymmetries and estimate the depth and type of sources that are responsible for exciting the solar p -modes.

2. OBSERVATIONS

To compare the asymmetry in velocity and intensity spectra, we computed spherical harmonic transforms (SHTs) of full-disk velocity and intensity images from the MDI instrument on board the *Solar and Heliospheric Observatory (SOHO)* (Scherrer et al. 1995). These SHTs were gap filled, Fourier transformed to make power spectra, shifted in frequency according to a solar rotation law, and averaged over the angular order m . To simplify the comparison, we chose the days 1996 July 21–23, for which simultaneous velocity and intensity images were available. The results for oscillations of angular degree $l = 200$ are shown in Figure 1.

From these two power spectra that have been normalized with respect to the maximum power, we see that the p -mode peaks of the velocity spectrum have negative asymmetry (more power on the low-frequency end of the peak), while the peaks of the intensity spectrum have positive asymmetry (more power on the high-frequency end of the peak). In the velocity spectrum (Fig. 1a), the asymmetry is strongest for low-frequency (low radial order) modes and becomes negligible around and above the acoustic cutoff frequency (≈ 5.2 mHz). However, the asymmetry in the intensity oscillations (Fig. 1b) increases with frequency for modes below the acoustic cutoff frequency and then gradually decreases at higher frequencies. The intensity spectrum shows a higher noise level as compared with the velocity spectrum.

Figure 2 shows the results with the model of the additive background subtracted. A notable shift in the peaks at the high-frequency part of the intensity spectrum is seen in relation to the same part of the velocity spectrum. This frequency shift is particularly strong at and above the acoustic cutoff frequency.

The other modes in the medium- l range (50–300) and the high- l range (300–1000) show similar properties of line asymmetry. While the degree of asymmetry varies across the spectrum, we have not yet detected a change in the sense of

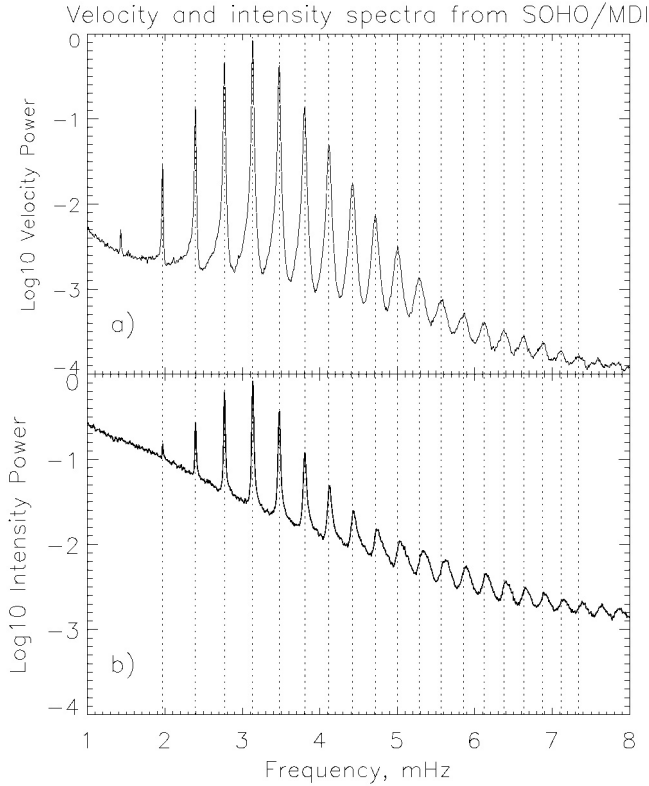


FIG. 1.—Normalized power spectra for solar oscillations of angular degree $l = 200$: (a) Doppler velocity and (b) continuum intensity for the same 3 day period 1996 July 21–23. The leftmost peak of the velocity spectrum corresponds to the f -mode. The other peaks of both spectra correspond to acoustic (p) modes of radial orders 1–21 (left to right). The vertical dotted lines in both panels indicate the locations of the p -mode maxima in the velocity power spectrum, to show that a relative shift in frequency occurred at and above the acoustic cutoff frequency (≈ 5.2 mHz).

asymmetry with l . For $l = 200$ and higher, there is a reversal of asymmetry for the f -mode in the velocity and intensity spectra, just as in the case of p -modes.

3. WHY IS THE ASYMMETRY REVERSED?

3.1. Numerical Model of Mode Excitation

We assume that solar acoustic waves are generated by turbulence in the convection zone and apply Lighthill's (1952) method, in which the acoustic sources of various multipole orders are transferred to the right-hand side of the wave equation, to calculate the velocity and pressure perturbations. We also assume that the observed intensity variations recorded by the MDI instrument correspond to Lagrangian pressure (or temperature) perturbations (Duvall et al. 1993; Abrams & Kumar 1996).

The background state is assumed to be spherically symmetrical, and all the perturbations are time harmonic; dissipation is modeled by viscous damping. Then, using a standard decomposition onto spherical harmonics (Gough 1993), we transform Lighthill's equations of motion, continuity, and energy (the full nonadiabatic problem is at least of the fourth order) into a simplified single second-order wave equation:

$$\frac{d^2 \Psi}{dr^2} + \left[\frac{\omega^2 - \omega_c^2}{c^2} - \frac{l(l+1)}{r^2} \left(1 - \frac{N^2}{\omega^2} \right) \right] \Psi = S(f, q), \quad (1)$$

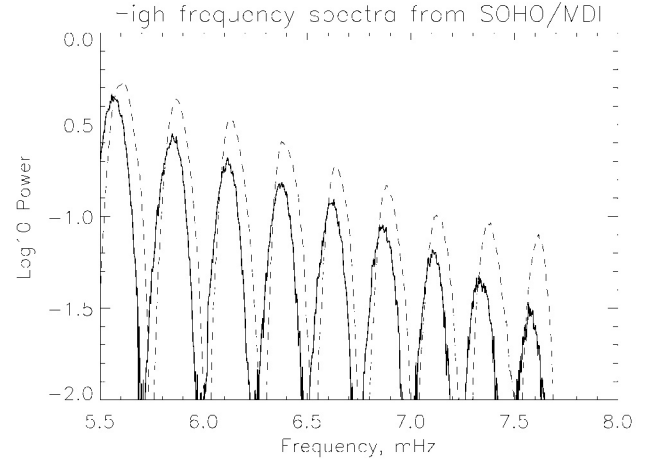


FIG. 2.—Normalized high-frequency velocity (solid curves) and intensity power spectra (dashed curves) of Fig. 1, with the model of the background subtracted. The relative shift in frequency is apparent.

where Ψ is proportional to the Lagrangian pressure perturbation δp (Gough 1993); r is the radius; ω is the frequency; ω_c is the acoustic cutoff frequency; c is the equilibrium sound speed; N is the equilibrium buoyancy frequency; and S is a combination of source terms that include the fluctuating Reynolds stress force, f , and the mass source, q . In this research, we consider a source given in equation (2) that is a combination of a monopole term (mass source) and a dipole term (Unno 1964). The dipole part results from when a monopole source is in a stratified medium and also from the radial and horizontal components of the Reynolds stress force. The radial component is more dominant than its horizontal counterpart for data of medium angular degree l . The expression for S is proportional to the sum of q , f , and their respective derivatives with respect to r . This type of composite source gives a good match with the MDI intensity and velocity data and is given by

$$S(r, \omega) = \left(c_1 \frac{dS_2}{dr} + c_2 S_2 \right) + \left(c_3 \frac{dS_1}{dr} + c_4 S_1 \right), \quad (2)$$

where c_1, c_2, c_3 , and c_4 depend on the solar model; S_1 is a source that contains the mass term and the horizontal component of the Reynolds stress force; and S_2 contains the radial component of the Reynolds stress force. S_1 scales as ω^{-2} , while S_2 does not contain ω explicitly, as discussed in Kumar (1994).

The Green's function $G_\Psi(r, r_s)$ of equation (1) for a delta-function source at $r = r_s$, using a standard solar model of Christensen-Dalsgaard et al. (1996), is found numerically using finite differences. The Sommerfeld radiation condition is applied above the upper turning point to ensure outgoing waves, and $G_\Psi(r, r_s) = 0$ at $r = 0$, as the perturbations are negligible much below the lower turning point. Damping is added by making the frequency complex, with the imaginary part having the damping coefficient. Since the source is close to the surface, where dissipative effects vary with position, the damping coefficient is a function of position. Two kinds of damping—spatial, similar to Abrams & Kumar (1996), and temporal—were investigated. It is found that they have very little effect on line asymmetry; damping basically affects the line width. The resulting system is a complex tridiagonal matrix equation that is solved by a standard routine. To compare with the observations, we multiplied the Green's function with a

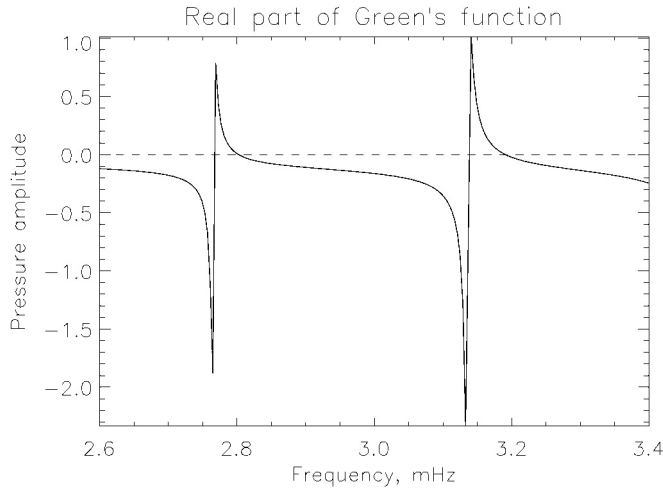


FIG. 3.—Real part of the normalized Green's function for solar p -modes of angular degree $l = 200$ produced by a composite source located at a depth $d = 75$ km beneath the photospheric level and an observing location $r_{\text{obs}} = 300$ km above the photosphere, where the observed spectral line is formed, for pressure perturbation. The dashed line corresponds to the zero points.

suitable source function and then added noise that was correlated with this source in a frequency-dependent manner.

3.2. Effect of Correlated Noise

For the solar potential of the simplified model, the real part of the Green's function for the pressure perturbation is calculated from equation (1) and shown in Figure 3. It has been normalized with respect to its maximum value. The imaginary part looks similar. The dashed line in Figure 3 corresponds to points of zero amplitude, which result when there is no driving by the source.

The Lagrangian perturbations are then calculated from the Green's function for a single source location and source type by multiplying it by a suitable source function and adding solar noise. The noise is assumed to consist of a part $c_p(\nu)$ that is correlated with the source function $s(\nu)$, while $n_p(\nu)$ forms the uncorrelated additive background. One then obtains for the pressure perturbation

$$p(\nu) = s(\nu)[c_p(\nu) + G_p(\nu)] + n_p(\nu), \quad (3)$$

and the velocity perturbation is found in a similar manner. Equation (3) is a simple model of the observed solar signal, which includes the correlated noise. Here G_p is proportional to G_Ψ .

The asymmetry in velocity and intensity power spectra is of an opposite sense because a component of the solar noise that is correlated with the source is present. The correlated component of the noise is below a certain threshold to preserve the asymmetry obtained by the above model in the velocity power spectrum, but it is large enough (i.e., above a certain threshold) to reverse the asymmetry in the intensity spectrum. The source position r_s from the origin is kept fixed, and the power spectrum is computed from equation (3) for the pressure perturbation. It is found that the correlation $c_p(\nu)$ reverses the asymmetry found in $G_p(\nu)$ when computing the power spectrum, as seen in Figure 4b. This is due to the fact that c_p shifts the zero points in $G_p(\nu)$. The uncorrelated noise plays no role in the reversal of asymmetry.

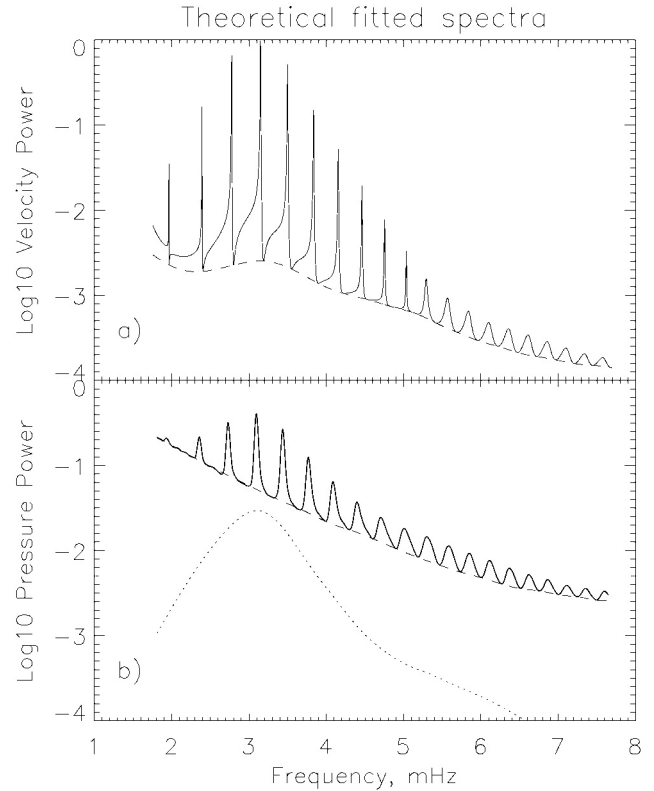


FIG. 4.—Normalized theoretical power spectra for solar p -modes of angular degree $l = 200$ produced by a composite source: (a) velocity spectrum (solid curve) with additive uncorrelated noise (dashed curve) and (b) pressure spectrum (solid curve) with additive correlated noise (dotted curve) and uncorrelated noise (dashed curve). The normalized correlated noise is multiplied by a factor of 5.

The intensity and velocity fluctuations are computed from the absorption line that is formed at a particular height in the solar atmosphere. The spectral line is affected by the p -mode oscillations and the solar granulation, which modulate and shift the line. It is thus the granulation overshoot that forms the correlated component of the noise, as it transports the effect of the source directly onto the line in the atmosphere. It also excites the solar oscillations in the intergranular lanes (Rimmele et al. 1995).

Without adding correlated noise, no reversal in asymmetry can be brought about between intensity and velocity in this simplified second-order problem. The full problem, incorporating nonadiabatic effects and radiative transfer in an inhomogeneous turbulent medium, is at least of the fourth order and was discussed in Kumar (1994). However, the full problem remains unsolved and is a subject of future investigation. The effect of correlated noise may be built into the framework of the general problem, but it is not present in the simplified second-order equation. Therefore, we add noise to our solution.

For the theoretical velocity power spectrum (Fig. 4a) corresponding to a delta-function source, the bound states (modes below the acoustic cutoff frequency ≈ 5.2 mHz) show marked asymmetry, which decreases with increasing frequency, while for the pressure power spectrum (Fig. 4b), their asymmetry increases with frequency. The peaks of the bound states are close to the eigenfrequencies if damping is small, as is the case for p -modes. The leaky states (modes above the acoustic cutoff frequency) have lesser asymmetry, and their peaks are mainly determined by the source position. They convey little infor-

mation about the solar cavity as compared with the bound states. In Figure 5 we capture the high-frequency shift that is present in the observations. Comparing the theoretical profiles with those of the observations, we find from Figures 1 and 4 that the profiles differ from the observations close to 3 mHz. Also, from Figures 2 and 5 we find that the power contrast (ratio of the maximum to minimum power) for the velocity spectrum is well reproduced but that for the pressure it is smaller than in the observations. This is due to the fact that we have used a simplified model of mode excitation and correlation. For simplicity, the correlation coefficient c_p has been assumed to be a constant. Pressure and velocity perturbations for sources extended over a range of depths can then be calculated from the respective Green's function by linear superposition.

It is important to note that the narrow range of the acoustic source depth (75 ± 50 km) that is found by comparing the theoretical and observed spectra coincides with the region of superadiabatic convection in the solar model. This region represents the highly unstable upper boundary layer of the convection zone, where the convective motions are most violent. The extent of the source was determined by comparing the high-frequency peaks of the theoretical spectra with those of the observations (Kumar & Lu 1991), for a range of source depths.

3.3. Effects of Source Type and Source Location

The reversal of asymmetry can also be brought about by changing the source location r_s or changing the source type. The asymmetry reverses whenever the source crosses a node of the eigenfunction. Moving the source deeper and keeping everything else fixed will reverse the asymmetry. Likewise, changing the source type (e.g., monopole to dipole) also reverses the asymmetry. However, without adding correlated noise, these effects reverse the asymmetry in both the velocity and the pressure spectra simultaneously. This does not explain the puzzle.

4. CONCLUSION

In this Letter, we have given a possible explanation for the puzzle regarding the opposite sense of asymmetry between intensity and velocity power spectra. This will have an implication on the fitting and determination of eigenfrequencies from the observed spectra, which will in turn affect the inversions.

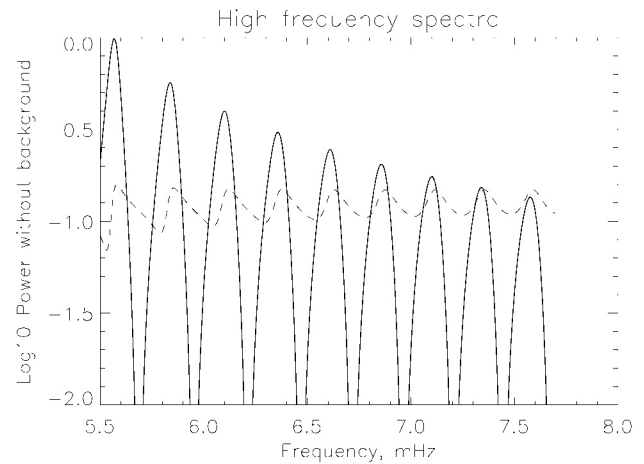


FIG. 5.—Normalized theoretical high-frequency velocity (*solid curves*) and pressure power spectra (*dashed curve*) of Fig. 4, with no additive uncorrelated noise. Correlated noise with coefficient c_p greater than a threshold value of 0.04 is responsible for the relative frequency shift that is present in the observations.

From our model we see that the intensity and velocity power spectra have an opposite sense of asymmetry, because the solar noise is partly correlated with the source that is responsible for exciting the solar oscillations. The solar noise is made up of two parts: one is correlated to the source, and the other is an additive uncorrelated background. This also explains the appreciable frequency shift at and above the acoustic cutoff frequency for the high-frequency pseudomodes, which are in fact responsible for the asymmetry of the bound states.

For a composite (monopole and dipole) source, the source depth is found to be in a thin layer 75 ± 50 km below the photosphere. It is remarkable that the theoretical spectra match the observations when the source is placed within the superadiabatic layer, thus pinning down the location, extent, and nature of the source.

We wish to thank T. Duvall, R. Bracewell, D. Gough, Å. Nordlund, S. Jefferies, T. Appourchaux, and S. Vorontsov for useful discussions. This research is supported by SOI-MDI NASA contract NAG5-3077 at Stanford University.

REFERENCES

- Abrams, D., & Kumar, P. 1996, *ApJ*, 472, 882
 Christensen-Dalsgaard, J., et al. 1996, *Science*, 272, 1286
 Duvall, T. L., Jr., Jefferies, S. M., Harvey, J. W., Osaki, Y., & Pomerantz, M. A. 1993, *ApJ*, 410, 829
 Gabriel, M. 1992, *A&A*, 265, 771
 Gough, D. O. 1993, in *Astrophysical Fluid Dynamics*, ed. J. P. Zahn & J. Zinn-Justin (Amsterdam: Elsevier), 399
 Kumar, P. 1994, *ApJ*, 428, 827
 Kumar, P., & Lu, E. 1991, *ApJ*, 375, L35
 Lighthill, M. J. 1952, *Proc. R. Soc. London*, A211, 564
 Nigam, R., Kosovichev, A. G., & Scherrer, P. H. 1997, in *Proc. IAU Symp.* 181, *Sounding Solar and Stellar Interiors*, ed. J. Provost & F.-X. Schmider (Dordrecht: Kluwer), in press
 Rimmele, T. R., Goode, P. R., Harold, E., & Stebbins, R. T. 1995, *ApJ*, 444, L119
 Roxburgh, I. W., & Vorontsov, S. V. 1995, *MNRAS*, 272, 850
 Scherrer, P. H., et al. 1995, *Sol. Phys.*, 162, 129
 Unno, W. 1964, in *Trans. IAU XIIB* (New York: Academic), 555